DOI: 10.12737/1024-6177-2019-64-5-42-47

Yu.A. Kurachenko[1], H.A. Onischuk[2,3], Eu.S. Matusevich[3], V.V. Korobeynikov[4]

HIGH-INTENSITY BREMSSTRAHLUNG OF ELECTRON ACCELERATOR IN PHOTONEUTRON AND RADIOISOTOPES PRODUCTION FOR MEDICINE

1. Russian Institute of Radiology and Agroecology, Obninsk, Russia. E-mail: ykurachenko@mail.ru;
2. Rosatom Technical Academy, Obninsk, Russia;
3. Obninsk Institute for Nuclear Power Engineering, NRNU MEPhI, Russia;
4. A.I. Leypunsky Institute for Physics and Power Engineering, Obninsk, Russia

Yu.A. Kurachenko – Chief Researcher, Dr. Sci. Phys.-Math.; H.A. Onischuk – Postgraduate Student;
Eu.S. Matusevich – Professor of MEPhI, Dr. Sci. Phys.-Math.; V.V. Korobeynikov – Chief Researcher, Dr. Sci. Phys.-Math.

Abstract

Purpose: To study the binary possibility of using the available linear electron accelerators for the neutron therapy and radioisotopes production. For both applications, calculations were performed and the results were normalized to the characteristics of the Mevex accelerator (average electron current 4 mA at a monoenergetic electron beam 35 MeV). It turns out that the production of both photoneutrons and radioisotopes is effective when using bremsstrahlung radiation generated in the giant dipole resonance of a heavy metal target.

Material and methods: The unifying problem for both applications is the task of target cooling: at beam power ~ 140 kW, half of it or more is deposited directly in the target. Therefore the liquid heavy metal was selected as a target, in order to conjoin high thermohydraulics quality with maximal productivity both bremsstrahlung radiation and photoneutrons. The targets were optimized using precise codes for radiation transport and thermohydraulics problems. The optimization was also carried out for the installations as a whole: 1) for the composition of the material and configuration of the photoneutron extraction unit for neutron capture therapy (NCT) and 2) for the scheme of bremsstrahlung generation for radioisotopes production.

Results: The photoneutron block provides an acceptable beam quality for NCT with a high neutron flux density at the output ~$2 \cdot 10^{10}$ $cm^{-2}s^{-1}$, which is an order of magnitude higher than the values at the output of the reactor beams that worked in the past and are currently being designed for neutron capture therapy. As for radioisotopes production, using optimal reaction channel (γ, n) 43 radioisotopes in 5 groups were received. For example, by the $Mo^{100}(\gamma,n)^{99}Mo$ reaction the precursor ^{99}Mo of main diagnostic nuclide ^{99m}Tc with specific activity ~6 Ci/g and total activity of the target 1.8 kCi could be produced after 1 day irradiation exposure.

Conclusion: The proposed schemes of neutron and bremsstrahlung generation and extraction have a number of obvious advantages over traditional techniques: a) the applying of the electron accelerators for neutron production is much safer and cheaper than to use conventional reactor beams; b) accelerator with the target, the beam output unit with the necessary equipment and tooling can be placed on the territory of the clinic without any problems; c) the proposed target for NCT is liquid gallium, which also serves as a coolant; it is an "environmentally friendly" material, its activation is rather low and rapidly (in ~4 days) falls to the background level.

Key words: *industrial electron accelerator, bremsstrahlung, photoneutrons, neutron capture therapy, radioisotopes for medicine*

Article received: 21.05.2019. Accepted for publication: 10.07.2019

Introduction

Radiation therapy, being one of the three main methods of oncology treatment (surgery, chemotherapy and radiotherapy), is not inferior to its role to this day both in terms of the rate of development and the breadth of application. It becomes increasingly selective, hitting the target with minimal exposure to healthy tissue. The most indicative in this respect is proton therapy, which allows relatively simple changes in the energy, intensity and diameter of the proton beam, which makes it possible to move the Bragg peak (maximum absorbed energy) in the tissue, supplying the dose conformally to the tumor using the gantry beam rotation system (see for example [1]). The use of neutrons, allowing the therapy of certain radioresistant tumors, apparently, is selective only in neutron capture therapy (NCT). The traditional source of neutrons for NCT are neutron beams of research reactors, and a huge seventy-year experience of success and failure has accumulated in this direction. This paper presents the results of long-term studies of the applicability for NCT the photoneutrons generated by the target of a powerful electron accelerator in the region of giant dipole resonance. In addition to the neutron beam modernization, the possibility of radioisotopes production by bremsstrahlung of the same accelerator is investigated. In general, the possibilities of photoneutrons for radiation therapy are undeservedly passed over in the literature. As an exception, we note the review [2], which analyzes photoneutrons arising from high-energy radiation therapy in the materials of the accelerator head and the patients' environment; these photoneutrons are traditionally and fairly treated as a harmful factor.

A powerful photoneutron source for medicine was considered in our paper [3]. In [4], the optimal configuration of the photoneutron beam extraction and focusing unit for neutron capture therapy was obtained, and in [5, 6] the thermohydraulics of the composite flow target W + Ga (coolant) and the beam applicability for radiation therapy were studied. The stationary fragment of the target is a matrix of refractory tungsten, through which gallium flows, allows sharp increase in the yield of photoneutrons in comparison with the target only from gallium. To normalize the calculation results, an average current 4 mA of the available Mevex industrial accelerator [7] was taken at electron energy 35 MeV.

Natural gallium is represented by two isotopes: ^{69}Ga (60.1 %) + ^{71}Ga (39.9 %). It is a low-melting metal (m_p = 29.8 °C) with a density 5.904 g/cm^3 in the solid state and 6.095 g/cm^3 in the liquid state. When molten, gallium remains in the liquid phase at room temperature for a long time. In addition, gallium has a wide temperature range

of liquid phase (to ~ 2200°C), so the radiation heat in the target can be easily removed.

Activation of natural gallium occurs due to photoreactions and reactions under the action of intrinsic neutrons. The main processes: ^{69,71}Ga(γ, n)^{68,70}Ga, ^{69,71}Ga(n, 2n)^{68,70}Ga, $^{69.71}$Ga(n,γ)$^{70.72}$Ga lead to the short-lived isotopes ^{68}Ga ($T_{1/2}$ = 68.3 min), ^{70}Ga ($T_{1/2}$ = 21.2 min) and ^{72}Ga ($T_{1/2}$ = 14.1 h). Calculations show that when the neutron fields those are characteristic for the NCT are generated and when the working medium of the target is circulated, the total activity of gallium (for typical irradiation scenarios and the number of sessions) falls to the level of the natural background in a time not exceeding 4 days.

Material and methods

In the transport calculations (MCNP5 code [8]) and in the calculations of the radioisotopes generation the nuclear data library TENDL-2017 based on the TALYS-1.9 [9] program of nuclear reactions was used.

NCT beam modernization

For modernization, the beam removal unit version with the maximal output flux density was selected [6].

The beam extraction unit is an axisymmetric assembly of cylindrical and conical layers and has protective and collimative (a conic lead layer) functions, as well the function of the spectrum shifter destined to form epithermal spectrum required for NCT.

Figure 1 shows fragments of the beam extraction unit with collimation system: channel filled with spectrum shifter (1, lead fluoride PbF_2, also performs the function of a gamma filter); the channel is surrounded by a collimator (2, Pb, the main function is the neutrons slowing down and canalization). Zirconium hydride $ZrH_{1.8}$ (3) in the collimating system is a light shielding; the borated polyethylene and Cd plate 1 mm thick (4) at the channel outlet are a thermal neutron filter.

In the interaction of accelerated electrons with a massive metal target W+Ga, the main energy loss channel is bremsstrahlung. At electron energies above ~10 MeV, the bremsstrahlung radiation absorbed by the W and Ga nuclei generates neutrons in the (γ, n) reactions in the region of the so-called giant dipole resonance with relatively large cross-sections and neutron yield (fig. 2).

The combined flow target is a tungsten cylinder with cylindrical coolant channels. In this paper, the target is modernized: the cylinder is enclosed in a spherical tungsten housing filled with coolant. The thermohydraulic calculation for the new target configuration is illustrated in fig. 3. Note that out of 140 kW of beam power from 65 to 70 kW is deposited directly in the target. The maximum coolant temperature obtained with the STAR-CD® code [10] is presented in fig. 3 for one of the possible heat removal modes.

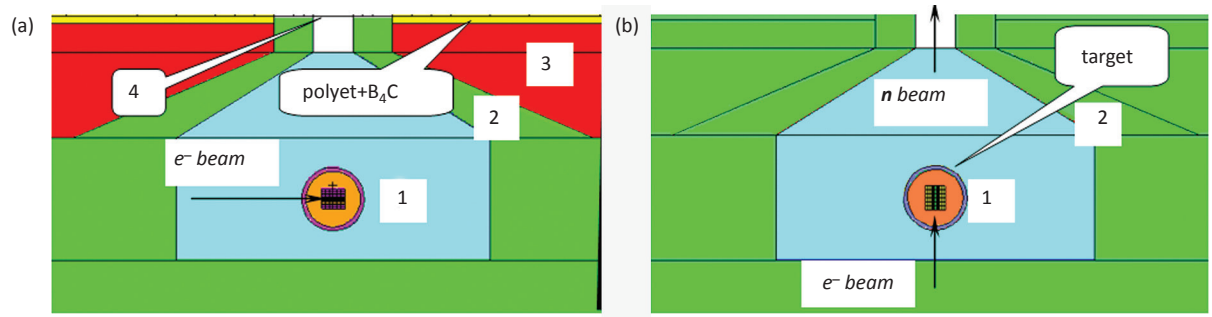

Figure 1. Axial sections of the axisymmetric beam extraction unit for NCT: start version from [6] (a) and its modernized version (b) (MCNP5 input visualization)

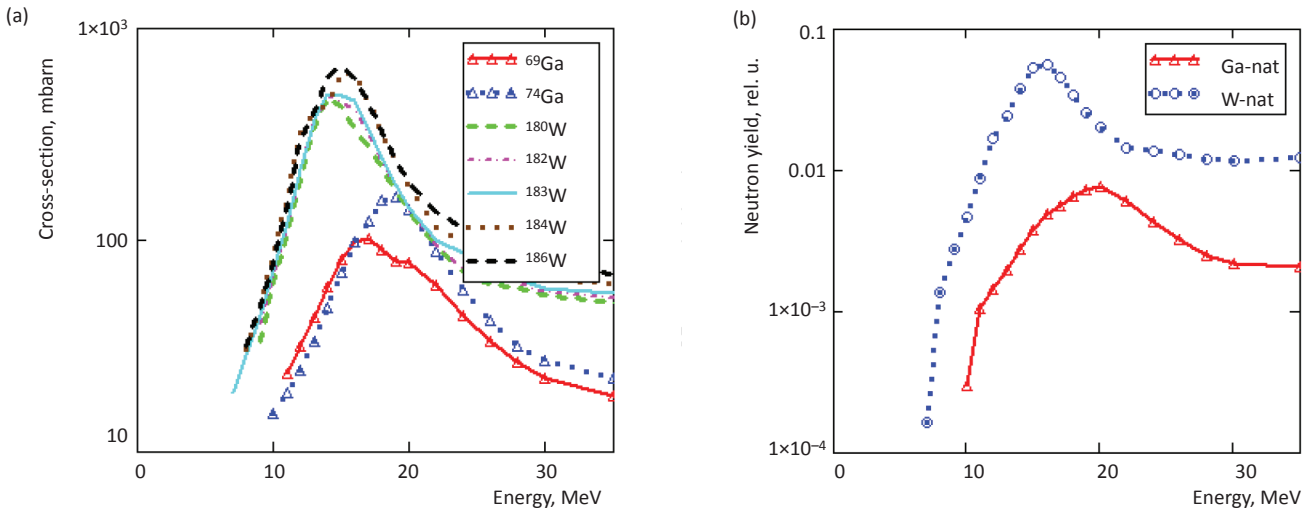

Figure 2. (a) – the total cross-section of neutron generation at the nuclei Ga and W; (b) – neutron yield from Ga and W; energy $E_\gamma \leq 35$ MeV (obtained using the TALYS library)

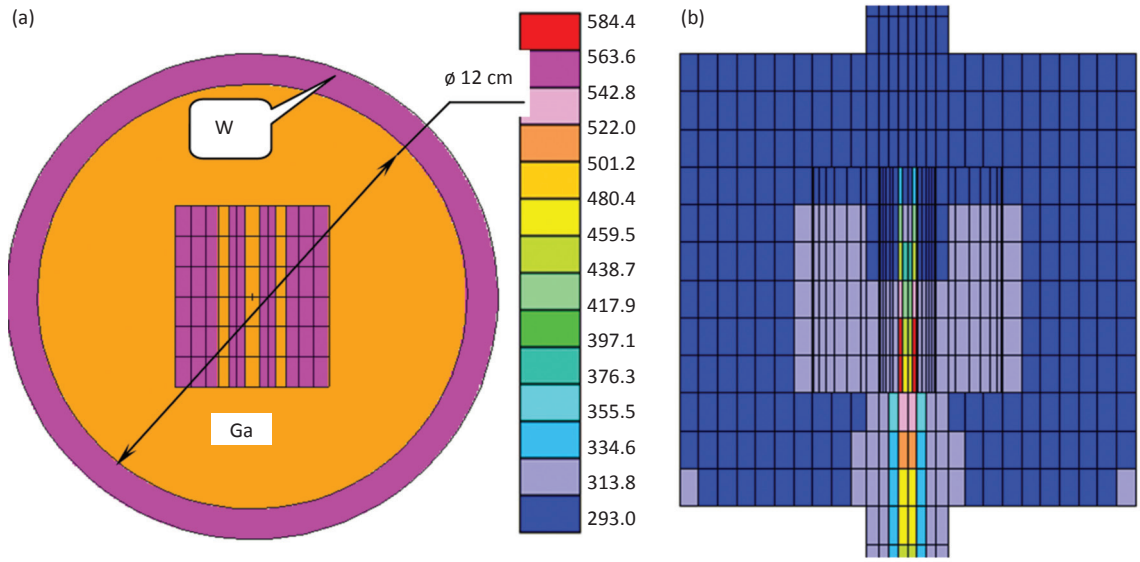

Figure 3. Models of the modernized target: (a) to calculate the energy release (MCNP5), (b) – to calculate the temperature field (code STAR-CD®). Coolant velocity 2 m/s, maximum coolant temperature 310 °C

Additional transport calculations made it possible to do justifiable changes in the configuration and material composition of the beam output unit, which led to safely increase the main functional, namely, the epithermal neutron flux density at the beam exit. The changes are as follows:

– the Cd plate at the outlet of the channel was removed, and the zirconium hydride was replaced by lead. The role of removed elements in reducing the thermal neutron flux is negligible: epithermal neutrons entering the tissue generate the backscattered thermal neutrons right close to the entrance; intensity these neutrons considerably exceeds the thermal neutron flux out of the channel;
– the combined flow target was deployed coaxial to the axis of the neutron beam exit and enclosed in a spherical tungsten case filled with gallium (fig. 3). This measure allowed to improve the heat sink (and decrease coolant maximal temperature), to increase the neutrons generation and to reduce the yield of "harmful" bremsstrahlung.

Radioisotopes production

Simplest model 1. For radioisotopes production (RP) according to the first model in (n,γ) reactions the conic moderator from the lead difluoride (PbF_2) has been replaced with heavy water (see fig. 1). The general configuration of the output block does not change; it is supposed to irradiate the samples at the channel output. It turned out that significant thermalization of a beam neutrons with such a small moderator depth (~ 0.5 m) could not be achieved: at total neutron flux density at beam exit $\Phi_{tot}=3.10\times10^{10}$ $cm^{-2}s^{-1}$ the thermal neutron flux density is only $\Phi_{th}=1.24\times10^{10}$ $cm^{-2}s^{-1}$. In the immediate vicinity of the target, the thermal neutron flux density reaches ~ 2.50×10^{10} $cm^{-2}s^{-1}$. Compared to the thermal neutron flux density in the reactor core, the hopelessness of the first model for RP is obvious.

Model 2: target with subcritical booster. The model consisting of a cylindrical tank filled with heavy water is presented in fig. 4. In the center of a tank there is a target, and on the periphery – subcritical assembly with $k_{eff} \leq 0.90$ (subcritical assembly with such k_{eff} does not require the control and protection system (CPS) during operation, [11], 2.2.2.15). Assembly consists of shortened fuel elements of the BN-600 reactor, cooled by heavy water. The moderator is also D_2O. As a result of calculation, rather leveled neutron field in a tank with heavy water is received. The maximum value of the total flux density $\Phi_{tot}= 6.19\times10^{11}$ cm^2s^{-1} is in immediate vicinity of the target, maximum of the thermal neutron flux density $\Phi_{th} = 3.09\times10^{11}$ $cm^{-2}s^{-1}$ is spaced away ~ 21 cm from a target. The neutron flux density has multiplied more than 10 times as compared to the results received for the first model. It is clear that if we increase the value of k_{eff} to the limit for subcritical assembly $k_{eff} \leq$ 0.98 [11], the flux characteristics will increase ~ 50 times with respect to the model 1 characteristics. But at the same time, it is necessary to use a complex CPS (at $k_{eff} \leq 0.90$ CPS is used only at the first criticality stage) and a bulky heat removal system. Perhaps, for some conditions the RP in (n, γ) reaction on model 2 is expedient, but it isn't possible to compete with reactor production.

Model 3: (γ, n) and (γ, p) reactions. It turned out that the model 3 is the most perspective, as yield of bremsstrahlung from a target is rather great. The studied cylindrical targets have been optimized to get maximal yield of bremsstrahlung when electron beam (radius

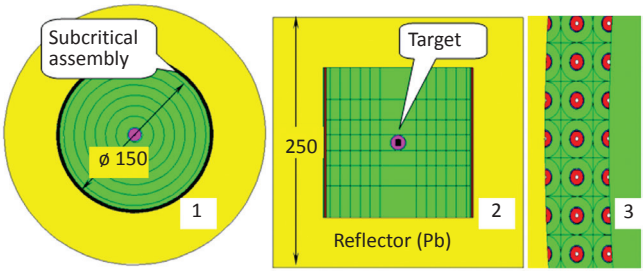

Figure 4. Radial (1) and axial (2) sections of model 2 composition; (3) – a fragment of a radial section with subcritical assembly in the form of a cylindrical layer adjacent to the wall. All dimensions are in cm

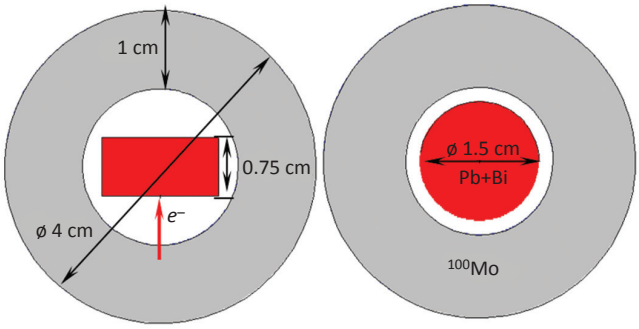

Figure 5. Sections of the spherical calculation model 3 of the ^{99}Mo production; arrow shows the direction of the electron beam (visualization of the MCNP5 input file)

0.5 cm) falls on an end face of the cylinder (table 1). At the chosen parameters of an electron beam the bremsstrahlung yield from optimal targets is almost identical for all heavy materials. The optimums in the target is quite flat, so when optimizing the dimensions of the target step of optimization was adopted to be equal to 0.25 cm. Average energy of the bremsstrahlung is in the region of a giant dipole resonance. For technological reasons the eutectic lead–bismuth is preferable as a target; in this case the alloy will be as well the coolant.

The efficiency of the model 3 can be shown by the example of the ^{99}Mo production by bremsstrahlung in the reaction ^{100}Mo(γ,n)^{99}Mo →^{99m}Tc. The cylindrical Pb-Bi target was enclosed in a spherical layer of parent nuclide ^{100}Mo (fig. 5). The ^{99}Mo production equation could be written as follow:

$$\frac{d\rho^{99}}{dt} = \sigma\Phi_0\rho^{100} - \lambda\rho^{99}, \quad (1)$$

where

ρ^{99}, ρ^{100} – nuclear density (10^{24} cm^{-3}) of daughter and parent nuclide;

$\sigma\Phi_0\rho^{100}$ – (γ, n) reaction rate (cm^{-3}s^{-1});

σ, Φ_0 – vectors of (γ, n) reaction cross-section (b) and photon flux density (cm^{-2}s^{-1}) with a length of tabular presentation on energy for a section and flux density;

λ – decay constant.

Integration (1) in the interval [0 – t_{irr}] of irradiation time taking into account the initial condition $\rho^{99}(t = 0) = 0$ gives the density of the produced nuclei [cm^{-3}]:

$$\rho^{99} = \sigma\Phi_0\rho^{100}(1 - \exp(-\lambda t_{irr}))/\lambda; \quad (2)$$

and the specific activity [Bq·cm^{-3}] of the produced isotope $A = \lambda\,\rho^{99}$ is:

$$A = \sigma\Phi_0\rho^{100}(1 - \exp(-\lambda t_{irr})). \quad (3)$$

Table 1

The target characteristics for model 3 mode of the RP

Target material	Tl	Pb	Bi	^{238}U	Pb + Bi (45%+55%)
R, cm	1.0	0.75	0.75	0.50	0.75
H, cm	1.0	0.75	1.0	1.0	1.5
Density, g/cm^3	11.843	11.342	9.79	19.05	10.6
Melting point, °C	304	324	271	1133	124
Bremsstrahlung yield, s^{-1}	1.29×10^{17}	1.32×10^{17}	1.34×10^{17}	1.25×10^{17}	1.33×10^{17}
Average energy, MeV	14.7	15.9	15.6	15.5	15.7

Let us compare our results with the data for photoreaction (γ,n) in [12] on producing ^{99}Mo at 14-kW electron accelerator with an energy of 40 MeV (i.e., the average current is 0.350 mA). For highly enriched (96 %^{100}Mo) sample with a mass 14.4 g at the 24 h exposure ~ 25 Ci or 1.74 Ci/g activity is produced [12]. Our data for the same exposure is 1.78 kCi and 5.96 Ci/g when the mass of the sample is 311 g, the average current 4 mA and 100 % ^{100}Mo target composition. Unfortunately, specific irradiation geometry [12] is not available. In [13] some information allows partial reconstruction the [12] data.

Analysis of (γ, p) total cross sections on target materials and proton yields [9] showed that in the given energy range $E_\gamma \le 35$ MeV the efficiency of radioisotope production will be small: both cross sections and proton yields are 2 orders of magnitude (or more) less than the corresponding values for neutrons.

Results and discussion

NCT beam quality

The "in air" functionals characterize the radiation field at the beam output without irradiated phantom and simplify the task of selecting the optimal configuration and composition of the output unit materials (without the laborious calculations of the "in phantom" functionals). It is assumed that if the "in air" characteristics do specific criteria worked out by the world community, then it is to be expected that the "in phantom" functionals will also satisfy the NCT requirements.

For comparison of the computed beams from a target of the electronic accelerator, the neutron beams' characteristics of exploited precedently for NCT reactors and projected medical reactor are attracted:

Table 2

Flux density, spectral characteristics and average energy of neutrons at the outlet of the reference (FCB MIT), exploited precedently (TAPIRO) and designed (MARS) reactor beams in comparison with characteristics of the photoneutron beams

		Φ_{tot}, cm^{-2}s^{-1}, 10^9	Φ_{epi}/Φ_{tot}, %	Φ_{fast}/Φ_{tot}, %	Φ_{therm}/Φ_{tot}, %	E^{Φ}_{aver}, MeV
Values, desirable for the NCT		≥ 1	~100	→ 0	→ 0	–
FCB MIT		4.2	data are absent			
MARS		1.24	81.6	13.4	5.0	0.0337
TAPIRO		1.07	73.6	6.5	20.0	0.00857
Photo-nuclear beams	best version [6]	18.5	74.9	25.1	0.014	0.0345
	current beam	27.8	73.3	21.6	5.11	0.0325

Table 3

NCT characteristics at the outlet of reactor and photonuclear beams: epithermal neutron flux density, "poisoning" of a beam with gamma radiation and fast neutrons, directivity

		Φ_{epi}, $cm^{-2}s^{-1}$, 10^9	D_γ/Φ_{epi}, sGy·cm², 10^{-11}	D_{fast}/Φ_{epi}, sGy·cm², 10^{-11}	J_{epi}/Φ_{epi} (flux-to-current)
Values, desirable for the NCT		≥ 1	< 2–5	< 2–5	≥ 0.7
FCB MIT		?	1.3	4.3	0.8
MARS		1.01	5.38	11.8	0.8
TAPIRO		0.788	6.77	8.49	0.8
Photo-nuclear beams	best version [6]	13.9	0.0407	15.9	0.8
	current beam	20.4	0.0262	13.4	0.8

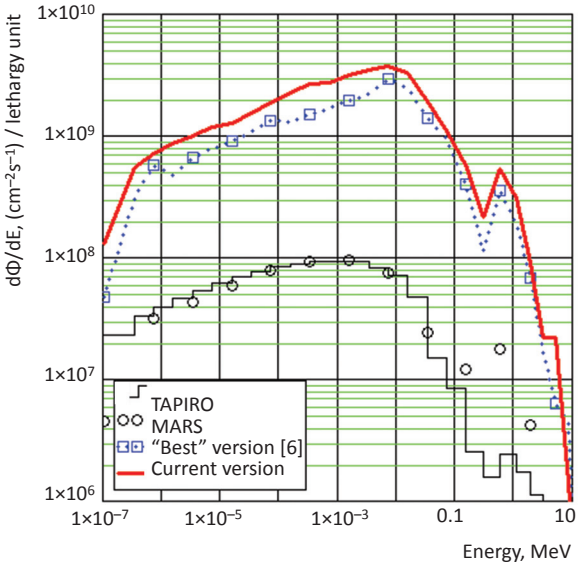

Figure 6. Neutron spectra at the outlet of the beam channel for NCT

– the FCB MIT beam, that is "reference" for the NCT (measurements, [14]), is decommissioned now;
– the epithermal column beam of the fast TAPIRO [15] reactor which was intended for application in the NCT (the calculation confirmed with measurements; the beam is decommissioned);
– the beam of specialized medical MARS reactor (calculation, [16]).

Base values of the "in air" characteristics for the compared beams are given in table 2. For photoneutrons, the data on "best" previous version [6] and updated now version of the removal unit (fig. 1) are submitted. Actual NCT criteria are presented in table 3. From the presented data it is necessary to draw a conclusion that according to criteria "in air" (or "for free beam") the offered photoneutron beam does not concede and even partly surpasses reactor beams for NCT. This conclusion is supported by the fig. 6 in which spectral characteristics of neutrons at the beam outlet are presented.

Table 4

The applied radioisotopes, obtained in the calculation on model 3 (for C, N, O and F, the parent isotope material is given in parentheses)

	Radioisotope	$T_{1/2}$	Activity, Ci	Specific activity, Ci/g
Positron emitters for PET				
1	**^{11}C** (Graphite)	20.39 min	140	2.22
2	**^{13}N** (Boron nitride)	9.965 min	45.9	0.718
3	**^{15}O** ($Be^{15}O$)	122.24 s	104	1.17
4	**^{18}F** ($Li^{18}F$)	109.77 min	313	4.05
5	^{38}K	7.636 min	139	5.50
6	^{44}Sc	3.97 h	2250	25.7
7	^{45}Ti	184.8 min	3310	24.9
8	^{49}Cr	42.3 min	3550	16.9
9	^{62}Cu	9.673 min	3030	11.6
10	^{64}Cu	12.700 h	4240	16.2
11	^{63}Zn	38.47 min	2090	9.97
12	^{65}Zn	244.06 d	20.1	0.0962
13	^{68}Ga	67.71 min	6140	35.4
14	^{78}Br	6.46 min	1820	20.0
15	^{80}Br	17.68 min	2480	27.3
Diagnostic radioisotopes				
1	^{51}Cr	27.7025 d	208	0.984
2	^{54}Mn	312.12 d	9.15	0.0433
3	^{74}As	17.77 d	220	1.31
4	^{73}Se	7.15 h	3960	28.2
5	^{85}Sr	64.84 d	20.6	0.277
6	^{97}Ru	2.9 d	2620	7.21

Radioisotopes list

Results of production calculation for some applied radioisotopes generated on model 3 in the same geometry (fig. 5) and under the same irradiation conditions are presented in table 4.

	Radioisotope	$T_{1/2}$	Activity, Ci	Specific activity, Ci/g
7	^{121}Te	19.16 d	123	0.672
8	^{139}Ce	137.64 d	30.9	0.156
9	^{140}Pr	3.39 min	3950	19.9
10	^{153}Gd	240.4 d	10.5	0.0453
11	^{157}Dy	8.14 h	6680	26.6
12	^{165}Er	10.36 h	5980	22.5
13	^{169}Yb	32.026 d	105	0.515
14	^{203}Hg	46.612 d	106	0.266
Radioisotopes for radionuclide therapy				
1	^{88}Y	106.65 d	11.9	0.0911
2	^{97}Ru	2.9 d	2620	7.21
3	^{103}Pd	16.991 d	126	0.359
4	^{153}Sm	46.50 h	487	2.21
5	^{159}Gd	18.5 d	3330	14.4
6	^{169}Er	9.40 d	314	1.18
7	^{186}Re	3.7183 d	5040	8.18
8	^{192}Ir	73.827 d	4870	7.34
Radioisotopes used in medical radionuclide generators				
1	^{99}Mo	65.94 h	1780	5.96
2	^{113}Sn	115.09 d	45.4	0.0985

Long-lived positron sources for space					
	Radioisotope	$T_{1/2}$	Activity, Ci	Specific activity, Ci/g	Comments
1	^{150}Eu	36.9 y	0.0385	0.000251	Long-term positron source, E_{aver}=0.22 MeV
2	^{152}Eu	13.54 y	0.528	0.00343	Long-term positron source, E_{aver}=0.30 MeV

Conclusion

The compactness of modern high-power accelerators and good controllability of the electron beam make it possible to provide binary application of bremsstrahlung generated in a giant dipole resonance for the neutrons and radioisotopes production. The proposed schemes of photoneutron generation and radioisotopes production have obvious advantages over reactor generation and production. First of all, this is ecological cleanliness: the coolant activity drops very quickly, there are no fission products in the installation, and the activation of the equipment is localized. Further, in this case the radiation and nuclear safety degree is immeasurably higher than that ones at reactor generation. Safety, as well as the relatively small dimensions and weight of the binary installation, allow it to be placed directly in the clinic. Finally, the flux density of epithermal neutrons (required for NCT) at the beam output is much higher than the neutron flux density at the output of the applied and projected reactor beams. Diversification by alternative generation of medical radioisotopes at the same facility improves its economy and expands opportunities. The high efficiency of ^{99}Mo generation, the precursor of the main diagnostic radioisotope ^{99m}Tc (~ 80 % of all procedures), is especially indicative.

REFERENCES

1. Kostromin SA, Syresin EM. Trends in accelerator technology for hadron therapy. Pis'ma v ECHAYA. 2013;184(10):1346-75. (in Russian).
2. Naseri A, Mesbahi A. A review on photoneutrons characteristics in radiation therapy with high-energy photon beams. Rep Pract Oncol Radiother. 2010;15(5):138-44. https://www.ncbi.nlm.nih.gov/pmc/articles/PMC3863143/pdf/main.pdf
3. Kurachenko YuA, Voznesensky NK, Goverdovsky AA, et al. New intensive neutron source for medical application. Medicinskaya fizika. 2012; 38(2):29-38. (in Russian).
4. Kurachenko YuA. Photoneutrons for neutron capture therapy. Izvestiya vuzov. Yadernaya energetika. 2014;4:41-51. (in Russian).
5. Kurachenko YuA, Zabaryansky YuG, Onischuk HA. Optimization of the target for photoneutron production. Izvestiya vuzov. Yadernaya energetika. 2016;3:150-62. (in Russian).
6. Kurachenko YuA, Zabaryansky YuG, Onischuk HA. Photoneutrons application for radiation therapy. Medical Radiology and Radiation Safety. 2017;62(3):33-42. (in Russian).
7. http://www.primaryprofile.com/Mevex-Corporation.
8. X-5 Monte Carlo Team. MCNP – A General Monte Carlo N-Particle Transport Code, Version 5. Volume I: Overview and Theory. LA-UR-03-1987. 2003; 484 p.
9. Koning A, Hilaire S, Goriely S. TALYS-1.9. A nuclear reaction program. ftp://ftp.nrg.eu/pub/www/talys/talys1.9.pdf. 2017;554 p.
10. STAR-CD®. CD-adapco Engineering Simulation Software – CAE and CFD Software.
11. NP-059-05: Nuclear safety rules for subcritical stands (PBYA PBS-2005). Federal rules and regulations on the use of nuclear energy. Moscow. 2005. (in Russian). https://files.stroyinf.ru/Data1/47/47666/
12. Ralph GB, Jerry DC, David AP, et al. A system of ^{99m}Tc production based on distributed electron accelerators and thermal separation. Nucl Technol. 1999;126:102-21.
13. Kuplennikov EL, Dovbnya AN, Tsymbal VA, et al. Estimation of the ^{99}Mo and ^{99m}Tc production on the CPhTI 9Be(d,n) generator. VANT. 2012;80(4):155-9. (in Russian).
14. Riley KJ, Binns PJ, Harling OK. Performance characteristics of the MIT fission converter based epithermal neutron beam. Phys Med Biol. 2003;48:943-58.
15. Agosteo S, Foglio Para A, Gambarini G, et al. Design of neutron beams for boron neutron capture therapy in a fast reactor. In: IAEA-TECDOC-1223, 2001:1-302.
16. Kurachenko YuA. Reactor beams for radiation therapy: quality criteria and computational technologies. Medicinskaya fizika. 2008;38(2):20-8. (in Russian).

For citation: Kurachenko YuA, Onischuk HA, Matusevich EuS, Korobeynikov VV. High-Intensity Bremsstrahlung of Electron Accelerator in Photoneutron and Radioisotopes Production for Medicine. Medical Radiology and Radiation Safety. 2019;64(5):42-7. (English).

DOI: 10.12737/1024-6177-2019-64-5-42-47